(Received 4 July 2025, Accepted 20 August 2025, Scheduled 7 September 2025)

A Non-Destructive Technique for Asphalt Compaction Measurement Using Dual-Ring Resonator Sensor

Mohammed K. Abbas[1, *], Raaed T. Hammed[1], Ali J. Salim[2], and Aduwati Sali[3, 4, *]

[1] *College of Electrical Engineering, University of Technology-Iraq, Iraq*
[2] *Microwave Research Group, College of Electrical Engineering, University of Technology, Baghdad 10066, Iraq*
[3] *Institute for Mathematical Research (INSPEM), UPM, Malaysia*
[4] *WiPNET Research Centre, Collage of Computer and Communication Systems Engineering Universiti Putra Malaysia (UPM), Serdang 43400, Selangor, Malaysia*

ABSTRACT: Traditional ways of measuring compaction of asphalt, which involve destructive coring, are labor-intensive, time-consuming, and cause permanent damage to the road. This paper presents a nondestructive alternative using a dual-ring resonator sensor (DRRS) integrated with a Vector Network Analyzer (VNA) to evaluate asphalt compaction. The sensor design takes advantage of the electric field that forms between the first and second rings. This field can penetrate the asphalt layer to a depth of up to 50 mm and responds to changes in compaction levels. By putting asphalt samples of different densities on the sensor and measuring scattering parameters (S-parameters), changes in the resonant frequency are shown. These shifts were correlated with asphalt's physical properties through empirical equations. The results showed that the resonant frequency and reflection coefficient (S_{11}) were -25.5 dB and 1.38 GHz, respectively, at a 75% compaction level. The frequency changed to 1.17 GHz at 100% compaction, and S_{11} was -17.6 dB. Increasing the compaction of asphalt makes the air gaps in the material smaller, which makes its permittivity higher. Calibration was performed to mitigate the influence of temperature on permittivity measurements, thereby improving compaction. Overall, this method provides a fast, precise, and nondestructive way to check the quality of asphalt, significantly enhancing road construction and maintenance processes.

1. INTRODUCTION

Accurate assessment of asphalt compaction is essential for ensuring the durability and safety of roads and streets. Although core sampling through drilling has been traditionally employed to measure compaction parameters, it is time-consuming and destructive. It can permanently undermine the pavement and asphalt's structural integrity, letting water penetrate beneath the asphalt layer into the soil below. This can cause the soil to sink and the pavement to break, as shown Fig. 1.

Microwave methods have been used successfully in many engineering fields, such as measuring soil compaction and classifying sand gradation. It is shown that they work well for non-destructive testing of engineering materials [1].

Different nondestructive methods have been suggested to get around these problems. Jilani et al. (2014) came up with an equivalent circuit model for a microwave sensor to test the dielectric properties of materials with high permittivity. Their research showed how resonant electric fields might improve the precision of measurements. It gives us a way to look at the intricate dielectric characteristics of biological tissues and other materials. The results showed that resonator-based sensors might be used for nondestructive testing in a variety of situations [2].

In 2016, Yasin et al. suggested using a top-loaded TM01 mode cylindrical dielectric resonator to measure the complicated permittivity of liquids. Their work focused on high-quality factor (Q-factor) resonators to improve measurement sensitivity and precision. This method offered a reliable approach for analyzing the dielectric properties of materials with high moisture content, which is critical for various sensing technologies [3].

In 2018, another study was conducted; Tiwari et al. [4] introduced a novel microstrip-based technique for the rapid determination of substrate permittivity, offering a simplified and efficient alternative to conventional methods.

Hoegh et al. (2019) looked at how Ground Penetrating Radar (GPR) could be used to study the soil below the surface, focusing on finding moisture and analyzing the layers of soil. The study used a multi-frequency GPR device to look at different types of soil and compare the results from the lab and field. The results showed that GPR is a good way to uncover differences in soil moisture and layer composition, and it could be useful for geotechnical and environmental investigations. The study also showed how important calibration models are for making data interpretation more accurate in soils that are not uniform [5].

Cao and Al-Qadi (2021) built a computational model to guess the dielectric characteristics of asphalt concrete that is not all the same. The goal of this model is to make GPR assessments for evaluating road infrastructure more accurate. The study looked at how different types of materials affect how electromagnetic waves respond by using both experimental data and numerical simulations. The study looked at things like fre-

* Corresponding authors: Mohammed K. Abbas (eee.20.03@grad.uotechnology.edu.iq); Aduwati Sali (aduwati@upm.edu.my).

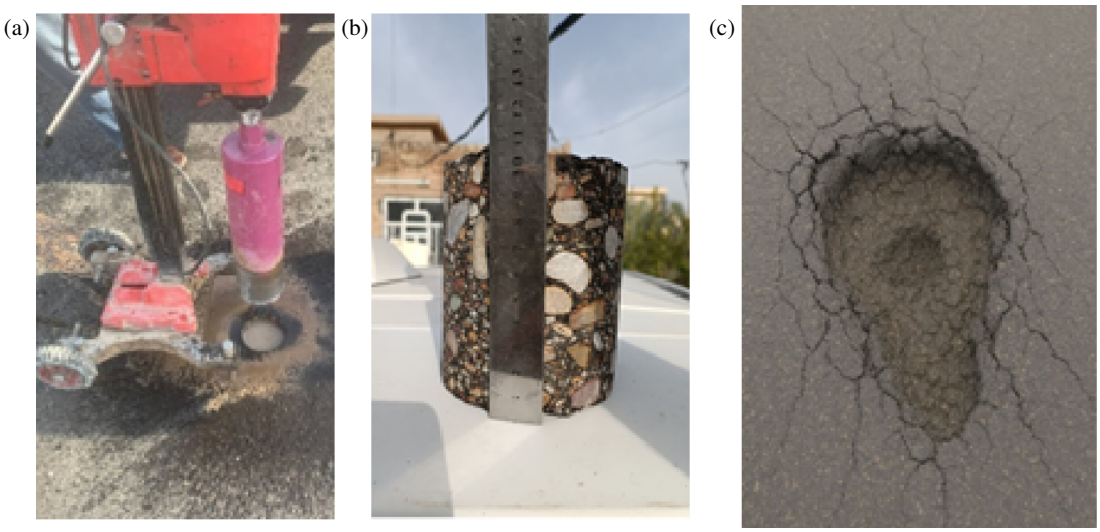

FIGURE 1. (a), (b) The traditional method used to measure the properties of asphalt by taking core samples through drilling, (c) the subsidence caused by water seepage into the subgrade soil.

quency, temperature, and moisture content to have a better idea of how dielectric characteristics fluctuate in different environments. The results showed that the model makes nondestructive pavement evaluations more accurate, which means that less expensive field sample is needed, and road infrastructure is less likely to be disrupted [6].

Zhang and Wang (2021) talked about and looked into how the dielectric characteristics of asphalt materials affect how GPR signals are interpreted. The study came up with a new way to estimate asphalt permittivity by combining lab observations with computer models. The study showed how different types of asphalt, such as the size of the aggregate and the amount of bitumen, affect changes in the dielectric constant. The results showed that accurately estimating permittivity makes GPR-based pavement thickness measurements more accurate, which lowers the number of mistakes made by nondestructive road evaluation methods [7].

Ren et al. (2024) developed an advanced material model for predicting asphalt performance based on electromagnetic wave interaction. The study combined GPR measurements with machine learning techniques to refine dielectric property estimations for asphalt pavements. The model was validated using real-world pavement structures, demonstrating improved accuracy in assessing material degradation and moisture infiltration. The findings suggest that integrating machine learning with GPR enhances the reliability of pavement health assessments, minimizing maintenance costs and improving long-term infrastructure monitoring [8].

Recently, Chen (2025) developed a reconfigurable spiral-shaped DGS sensor for nondestructive defect detection in dielectric composites by monitoring frequency shifts, demonstrating enhanced sensitivity and reduced blind spots — highlighting the potential of resonator-based microwave techniques for material evaluation [9].

Traditionally, asphalt properties are measured by extracting core samples for laboratory analysis. While this method is widely used, it is time-consuming, invasive, and often disrupts natural layers of the asphalt. To address these limitations, nondestructive testing (NDT) techniques have been explored. However, traditional methods like Ground Penetrating Radar (GPR) typically provide qualitative data, making it challenging to extract critical parameters such as delay times and phase differences, which are essential for accurately evaluating asphalt properties.

In this paper, a two-port sensor is utilized to overcome these challenges. This approach enables the calculation of frequency shifts and S-parameters to assess asphalt compaction, significantly reducing measurement complexity and processing time. Signals transmitted through the first port are received by a second port connected to a Vector Network Analyzer (VNA), allowing for precise measurement and analysis.

The objectives of this study are:

(1) To design a two-port sensor for evaluating the property of material under test (MUT).

(2) To measure asphalt compaction using a Vector Network Analyzer (VNA) as an alternative to traditional Ground Penetrating Radar (GPR).

2. DUAL-RING DESIGN

The methodology of this research consists of two main phases: sensor design, testing and developing a model for asphalt compaction measurement.

2.1. Design of a Dual-Ring Design

The proposed dual-port sensor, based on electric coupling between two rings, is constructed on an FR4 substrate characterized by a relative permittivity $\varepsilon_r = 4.3$, a thickness of $h = 1.6\,\text{mm}$, and a loss tangent equal to 0.027. The sensor has a rectangular substrate with side lengths $L_p = 128\,\text{mm}$ and $w_p = 80\,\text{mm}$. Fig. 2 illustrates the configuration of the sens-

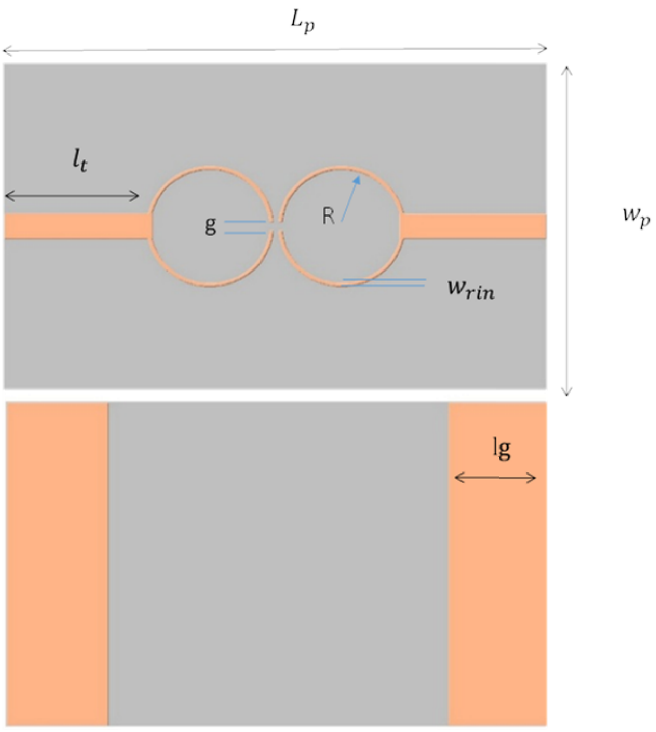

FIGURE 2. The proposed dual-ring sensor: front view and back view.

ing unit, where the sensor consists of three layers: the top layer from copper 0.03 mm features two rings and a transmission line; the bottom layer comprises two copper pieces separated by a gap; and the middle layer is the support substrate. The sensor design includes two straight connections, each 3.1 mm wide, integrated with a ring resonator to achieve a 50 Ω impedance via a 35 mm microstrip line.

The radius of the split-ring resonator equals 14 mm; the split-ring gap equals 2 mm; and the ground plane contains two parts of copper.

All related effective parameters are labeled in Fig. 2 and have the physical dimensions presented in Table 1.

TABLE 1. Optimum dimensions of the proposed sensor.

Parameter	Value [mm]	Parameter	Value [mm]
L_p	128	R	14
W_p	80	g	2
l_t	35	W_{rin}	1
l_g	24	W_f	3.1

The planar sensor operates as a resonant system based on the principle that wave characteristics change when interacting with a dielectric material. This interaction causes a shift in the resonance frequency and changes in S_{11} and S_{21} responses. After optimizing design parameters, S-parameters were recorded, as shown in Fig. 3, which illustrates the frequency response of the proposed sensor in air, that is, with no material placed on the sensing surface.

The resonant frequency is observed at 1.4 GHz, at which point the reflection coefficient is measured to be −18 dB.

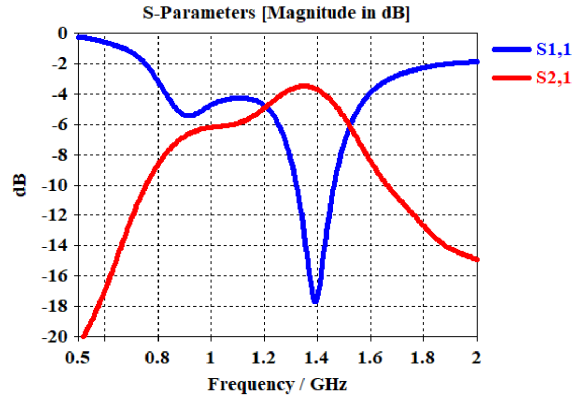

FIGURE 3. Simulated S-parameters response of the resonator in air (without any material under test).

2.2. Simulation Results

The operational principle of the sensor relies on the electric field generated between the rings, which penetrates the superstrate layer and interacts with the MUT. This interaction mechanism is illustrated in Fig. 4, where the field distribution demonstrates how the electric field extends into the material placed above the resonator. Following the completion of the sensor design using a double C-RING configuration, this section investigates the effect of both relative permittivity and MUT height, as that of asphalt, on the sensor's response through variations in dielectric properties.

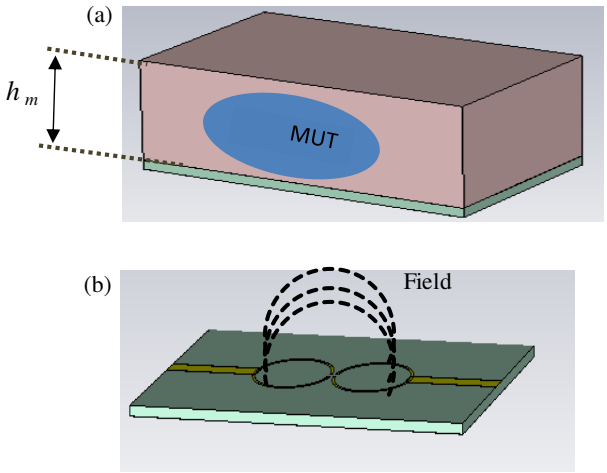

FIGURE 4. The electric field. (a) The height of the MUT, and (b) the field of the proposed sensor.

2.3. Perfect Selection of MUT Height

The effect of material under test (MUT) height on the frequency shift of the proposed sensor, utilizing a double C-RING configuration, is analyzed to study the compaction of the material under test (MUT) through dielectric properties, such as asphalt, when it is placed as a superstrate layer. In this context, f_r of the S-parameter represents the sensor's resonance frequency.

The performance of the sensor is strongly affected by the height of the sample. To investigate this effect, the height of the superstrate was varied, keeping its length and width equal

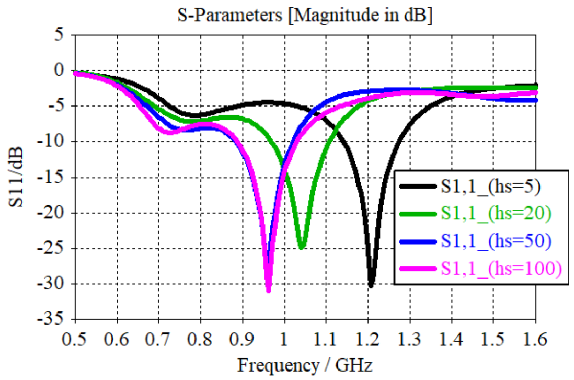

FIGURE 5. The simulated S_{11} response of the proposed sensor with MUT height parameter when permittivity 4.5.

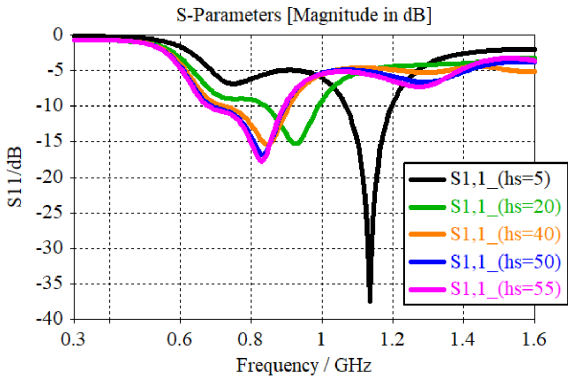

FIGURE 6. The simulated S-parameters response when permittivity is equal to 6.

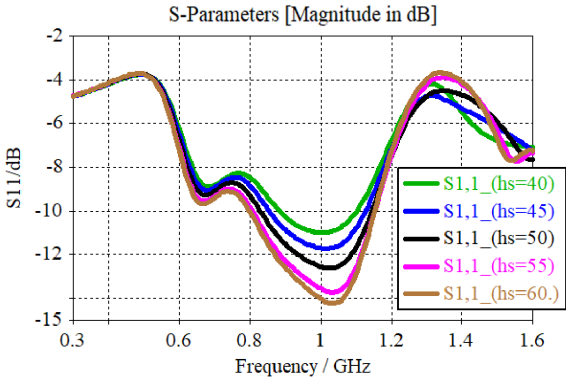

FIGURE 7. The simulated S_{11} response of the proposed sensor with MUT height parameter when permittivity 7.5.

to those of the sensor substrate. The permittivity of the asphalt samples was varied within a range of 4.5 to 7.5 [10]. For this analysis, the lowest, intermediate, and highest permittivity values were chosen to study the effect of sample height on the resonant frequency. The permittivity of the sample remained constant during each test. Three case studies were considered:

In the first case, the permittivity of the Material Under Test (MUT) is set to 4.5, and its thickness is varied from 5 to 100 mm. Noticeable shifts in the resonant frequency f_r are observed, as shown in Fig. 5. These variations in thickness significantly affect the frequency response, including the analysis of S-parameters and reflection coefficient.

The results indicate that the effect of sample height on resonance frequency and scattering parameters is noticeable up to 50 mm. Beyond this point, the changes are minimal, suggesting that the effective penetration depth of the electric field does not exceed 50 mm.

In the second case, when the Material Under Test (MUT) has a permittivity 6 (in the mid-range), the sample thickness was again varied from 5 mm to 100 mm. The sensor continued to show clear shifts in the resonant frequency, as illustrated in Fig. 6. However, similar to Case 1, the maximum effective sensing depth was found to be approximately 50 mm. Any further increase in height resulted in negligible changes in the frequency response, confirming the field penetration limit for this permittivity value.

The study revealed that with a permittivity of 6, and the maximum effective sample height reaches 50 mm, after which any additional increase has an insignificant effect.

In the third scenario, when the permittivity of the Material Under Test (MUT) is set to 7.5 (the highest value considered) and the sample thickness varied from 5 mm to 100 mm, noticeable shifts in the resonant frequency (f_r) are observed up to a thickness of 50 mm. Beyond this point, further changes in thickness result in minimal variation. As illustrated in Fig. 7, these thickness variations significantly affect the frequency response and the analysis of S-parameters, including the reflection coefficient. Once the sample height reaches 50 mm, the frequency shift becomes negligible, indicating that the sensor's electric field does not effectively penetrate beyond this depth.

After evaluating all three cases, the study confirms that significant variations in frequency shifts occur when the sample height is less than 50 mm. However, once the height reaches 50 mm, the changes in frequency shift become minimal. It indicates that 55 mm is the minimum height for MUT, beyond which the fringing field penetration saturates, and further height increases have a negligible effect, as shown in Fig. 8.

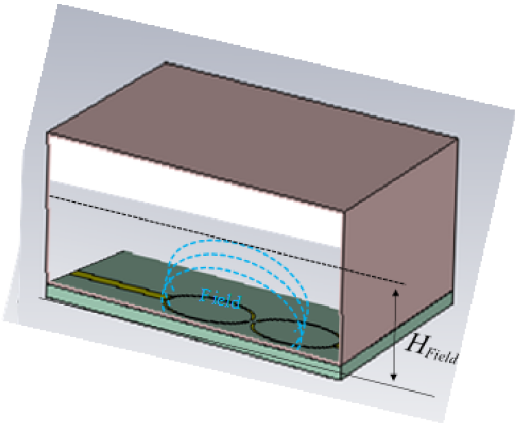

FIGURE 8. The depth of field is equal to 50 mm.

2.4. Effect of Permittivity on Signal Behavior

After analyzing the effect of sample height on sensor performance, we now examine how permittivity influences signal response. Permittivity plays a fundamental role in the interac-

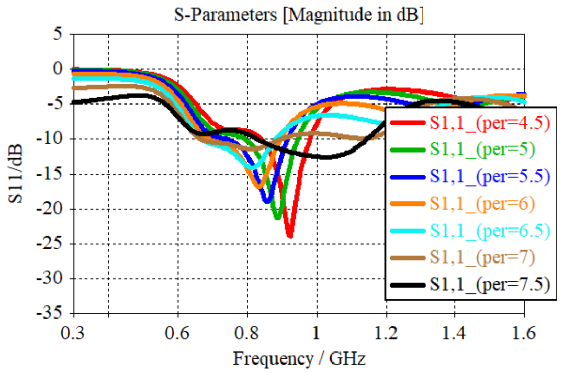

FIGURE 9. The simulated S_{11} response of the proposed sensor with permittivity when hs parameter is equal to 55 mm.

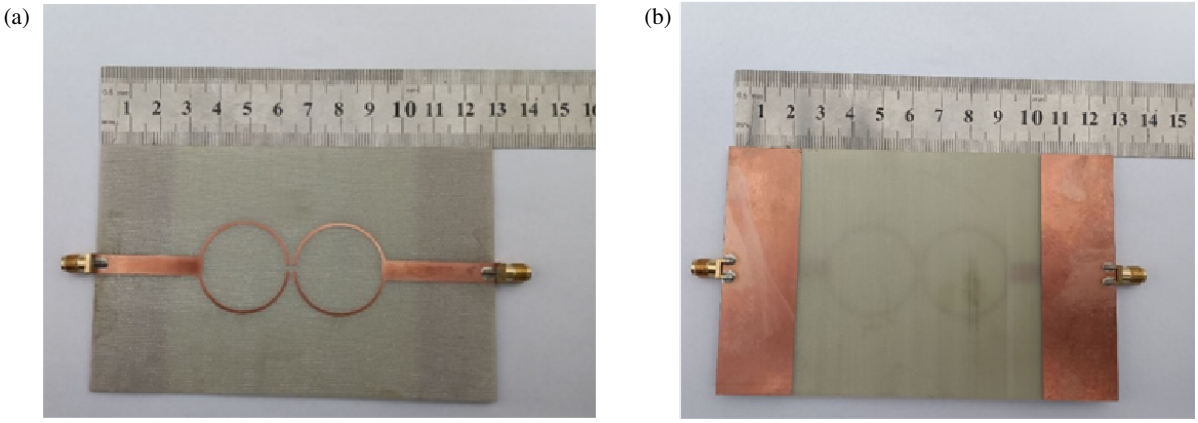

FIGURE 10. The fabricated sensor, (a) front view, and (b) back view.

tion between electromagnetic waves and the material under test (MUT), directly affecting three key parameters: resonance frequency shift (Δf_r), reflection (S_{11}), and transmission (S_{21}).

To understand these relationships, we maintained a constant sample thickness of 55 mm while varying the permittivity. When permittivity decreases, the resonant frequency shifts upward toward higher values, while the reflection coefficient shows improvement, as illustrated in Fig. 9.

The downward frequency shift with increasing permittivity will be utilized to measure asphalt compaction after the sensor is fabricated.

3. SENSOR FABRICATION AND MEASUREMENT RESULTS

Figure 10 shows the physical prototype, which is printed using a laser printer (LPKF S-103). The performance of the proposed sensor demonstrates that the design is accurate, reliable, and fully operational within the intended frequency bands. The S-parameter results of the proposed sensor, shown in Fig. 11, reveal a close alignment between the simulated and measured reflection coefficients, confirming the consistency and validity of the design.

It can be noted that both curves display sharp dips at certain frequencies, indicating good sensor performance in these frequency bands. The slight differences between the measured

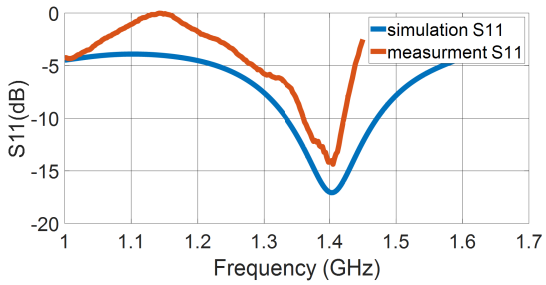

FIGURE 11. The simulated and measured S-parameters for the fabricated sensor.

and simulated results were observed, with S_{11} deviations due to an unspecified value for ε_r, losses in the SMA connector or both. The resonant frequency is 1.4 GHz, and the reflection coefficient is -18 dB.

4. COMPONENT OF ASPHALT MIXTURE

The 20 Kg of asphalt were analyzed and prepared according to the American Society for Testing and Materials (ASTM) specification, as shown in Table 2.

Previous research demonstrated that a dual crescent-shaped printed antenna could effectively classify asphalt mixture gradations based on electromagnetic response characteristics, val-

TABLE 2. Gradation and bitumen content of asphalt mix (sieve analysis).

Sieve Size [mm]	Passing Ratio [0–1]	Passing Weight [kg]	Mix Weight [kg]	Mix Ratio [0–1]
37.5	1.00	20.0	0.0	0.00
25	0.95	19.0	1.0	0.05
19	0.84	16.8	2.2	0.11
12.5	0.70	14.0	2.8	0.14
9.5	0.64	12.8	1.2	0.06
4.75	0.44	8.8	4.0	0.20
2.36	0.30	6.0	2.8	0.14
0.30	0.12	2.4	3.6	0.18
0.075	0.04	0.8	1.6	0.08
Bitumen content	0.04	0	0.8	0.04

FIGURE 12. Asphalt samples with varying levels of compaction: (a) an overview of the samples, (b) the experimental setup using the sensor and VNA to measure S-parameters, (c) minimum compaction at 72% and maximum compaction at 100%.

idating the use of printed antenna technology for mixture component analysis [1].

5. ASPHALT SAMPLING AND COMPACTION MEASUREMENT

The procedures for measuring the resonator's response to changes in asphalt compaction begin by preparing cubic asphalt samples with dimensions equal to or greater than the dimension of the resonator to ensure complete coverage. After incrementally compacting the samples and measuring their densities, each sample is securely placed on the resonator to maintain stable contact before the resonator is connected to the Vector Network Analyzer (VNA), as illustrated in Fig. 12. The reflection coefficient (S_{11}) and transmission coefficient (S_{21}) are then measured across a frequency range that encompasses

TABLE 3. Measurement results with different moisture percentages of water content at 20°.

Samples	Compaction	Density [kg/m^3]	f_r [GHz]	S_{11} [dB]	S_{21} [dB]	$\lvert S_{11}-S_{21}\rvert$ [dB]
Sample1	75%	1460	1.38	−2.5	−8.6	17.9
Sample2	87%	1708	1.27	−23.15	−8.7	17.47
Sample3	93%	1820	1.22	−20.55	−9.09	13.81
Sample4	96%	1878	1.19	−19.12	−9.31	12.83
Sample5	100%	1956	1.17	−17.6	−11.7	5.9

the resonator's operating frequency, noting any shifts in the resonant frequency and changes in the scattering parameters. Based on the relationship between the relative permittivity (ε) and density (ρ), the asphalt density is calculated and recorded in Table 3, containing sample number, resonant frequency, density, and scattering parameter measurements. Finally, a graph is plotted to visualize the correlation between resonant frequency (x-axis) and asphalt density (y-axis), providing a clear summary of the results, as shown in Fig. 13,

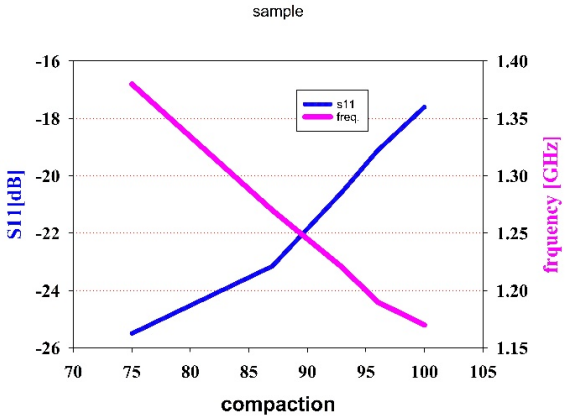

FIGURE 13. S-parameters and frequency shift vs compaction.

Table 3 shows the effects of various parameters on S_{21}, delay time, power, and phase as determined using VNA and MATLAB. For neural network training on soil moisture measurement, a test was done with an asphalt-plugged box.

The procedure involved collecting several data points by sending and receiving signals while adjusting the compaction of the testing box to vary between different readings of compaction level, and all measurements in Table 3 were performed at an ambient temperature of 20°C.

Although machine learning approaches, such as Long Short-Term Memory (LSTM) and U-Net, have strong potential to analyze data, in this paper, a simple linear regression model was developed due to the limited dataset, making it a more reliable and practical choice. Those deep learning methods could be applied in future work for asphalt compaction measurement and error classification with higher precision [11].

To estimate asphalt compaction in a simple and practical manner, a linear regression model was developed using resonance frequency (GHz) and reflection coefficient S_{11} (dB) as input variables. The resulting empirical Equation (1):

$$Compaction\,(\%) = 218.31 - 91.58 f_r + 0.66 S_{11} \quad (1)$$

with frequency in GHz and S_{11} in dB.

This model provides a straightforward way to predict compaction based on measurable microwave parameters without the need for destructive coring. To evaluate the model's accuracy, several statistical metrics were computed:

- Mean Absolute Error (MAE): 0.31%
- Mean Squared Error (MSE): 0.16%
- Root Mean Squared Error (RMSE): 0.40%
- Coefficient of Determination (R^2): 0.998

The high R^2 value indicates a strong correlation between the predicted and actual compaction values, confirming the reliability of the linear model for practical, nondestructive assessment of asphalt compaction in field applications.

The nonlinearity that was seen is because the samples were prepared by hand, which can cause variances in the distribution of aggregates and small differences in the size of the cubes, which can cause small differences in compaction.

The field calibration protocol consists of two components: temperature compensation and asphalt mixture calibration.

Temperature is the first part of compensation. Temperature has a direct effect on the permittivity of the asphalt mixture. If the temperature is not corrected for its effect, the resonant frequency will go down, and the bias in compaction estimation will go up. We did field calibration by testing the same samples again at 40°C instead of 20°C, as shown in Table 4. This comparison showed a clear drift in compaction values at higher temperatures compared to the reference measurements. It shows that we need a way to compensate the temperature.

A linear temperature compensation term was added to the empirical model in Equation (2):

$$Comp(\%) = 218.3 - 91.58 f_r + 0.66 S_{11} - \beta_t (T - 20) \quad (2)$$

TABLE 4. Field calibration results at different temperatures.

Samples	Compaction at 20°C	Compaction at 40°C	β_t
Sample1	75%	75.7%	0.0350
Sample2	87%	87.5%	0.0250
Sample3	93%	93.6%	0.0299
Sample4	96%	96.4%	0.0200
Sample5	100%	100.7%	0.0350

TABLE 5. Comparison between the proposed model and references.

Ref.	Device used	Application	Method, key features	Temperature Calibration	Limitations
[14]	Circular Ring Resonant for moisture sensing	Dielectric analysis for varying material	Analysis of frequency shifts using VNA	No	Penetrating is 6 mm;
[15]	Two-line transmission line technique and VNA	Permittivity Extraction of Wet Soil	S_{21} and S_{11}	No	It focuses on the S-Parameters and does not address Transmission Line length
[6]	GPR	Permittivity Extraction of asphalt	Reflection Amplitude Method	No	Requires GprMax simulation
[16]	Percometer and the probe.	Concrete and asphalt properties	Time delay and reflected signal	No	Requires a sheet of aluminum under the layer
[9]	Spiral-shaped DGS sensor	Dielectric defect detection	Reconfigurable with tunable notch via VNA	No	Requires biasing circuit for diode control
[17]	The dielectric constant test platform	Permittivity of asphalt core at different temperatures	Measures permittivity at varying temperatures	Yes	The model is Destructive and based on specific asphalt mixes from sampled
DRRS	**VNA**	**Asphalt compaction and thickness**	**Phase, *S*-parameters**	**Temperature and mixture considered**	**Penetrating is 50 mm**

where β_t is the thermal correction factor (%/°C) derived from the calibration process.

The average thermal correction factor was determined equal to (0.029%/C°).

In the asphalt mixture calibration protocol, a quantity of asphalt is collected directly from the paving machine, placed into cubic molds and compacted at different levels to represent realistic field conditions. The compaction level of each sample is determined, and both the frequency and S-parameter are measured using the DRRS sensor. These measurements are then used to update the empirical model parameters α, β, and γ. If it is not possible to collect asphalt samples before paving, three cores with different compaction levels are extracted from the finished pavement. Their compaction is determined, and the same parameters are measured to calibrate the model according to site-specific conditions, applying appropriate correction factors. The updated empirical model is expressed as Equation (3):

$$\begin{aligned} Compact.(\%) &= (218+\alpha)-(91.5+\beta)f_r \\ &\quad +(0.6+\gamma)S_{11}-0.029(T-20) \end{aligned} \quad (3)$$

6. COMPARISON WITH RELATED STUDIES AND SUGGESTIONS FOR FUTURE WORK

To inspect the performance of the sensor clearly, some comparisons between the proposed model and previous models reported in the references are summarized in Table 5. It is obvious that the proposed model can achieve more penetration, reaching up to 50 mm while [8] reaches only 6 mm, does not need a metal layer at the base to reflect signals, has a low profile, and can measure compaction. Both temperature calibration and asphalt mixture calibration have been considered in this study.

Future work could apply a Fuzzy Similarity approach, where asphalt mixtures are clustered by component ratios, and compaction is predicted from mixture data, temperature, resonance frequency, and S_{11}. This treats data as approximate sets with varying compatibility, enabling robust feature extraction, reduced computational complexity, and greater resilience to uncontrolled variations. The theoretical basis is detailed in [12].

DRRS sensor can be mounted directly on asphalt compaction rollers to provide continuous real-time feedback on compaction values during paving operations. The system wirelessly transmits data to mobile devices via Wi-Fi connectivity, enabling operators to monitor compaction progress instantly and adjust rolling patterns as needed [13].

7. CONCLUSIONS

The electric field generated between the two rings of a Dual Ring Resonator Sensor (DRRS) penetrates the asphalt layer to a maximum effective depth of approximately 50 mm for non-destructive measurement of asphalt compaction. Therefore, to ensure full interaction with the sensing field, the thickness of any asphalt, whether well-compacted or loose, must be at least 50 mm. As the compaction of the asphalt layer increases, the resonant frequency shifts downward, and the S_{11} value decreases. This is accompanied by a rise in relative permittivity attributed to the reduction of air voids within the asphalt mixture. Consequently, the permittivity increases noticeably. This phenomenon has been utilized in this study to measure asphalt compaction nondestructively, eliminating the need for core sampling or drilling.

REFERENCES

[1] Abbas, M. K., R. T. Hammed, A. J. Salim, and A. Sali, "A high-efficiency, indirectly-fed, dual moon-shaped printed antenna for measuring sand gradation," in *2024 IEEE 7th International Symposium on Telecommunication Technologies (ISTT)*, 31–36, Langkawi Island, Malaysia, 2024.

[2] Jilani, M. T., W. P. Wen, L. Y. Cheong, M. A. Zakariya, and M. Z. Rehman, "Equivalent circuit modeling of the dielectric loaded microwave biosensor," *Radioengineering*, Vol. 23, No. 4, 1038–1047, 2014.

[3] Yasin, A., F. Rehman, U. Naeem, S. A. Khan, and M. F. Shafique, "Top loaded TM01δ mode cylindrical dielectric resonator for complex permittivity characterization of liquids," *Radioengineering*, Vol. 25, No. 4, 714–720, 2016.

[4] Tiwari, N. K., S. P. Singh, and M. J. Akhtar, "Novel microstrip-based simplified approach for fast determination of substrate permittivity," *IEEE Transactions on Components, Packaging and Manufacturing Technology*, Vol. 8, No. 4, 660–669, 2018.

[5] Hoegh, K., R. Roberts, S. Dai, and E. Z. Teshale, "Toward core-free pavement compaction evaluation: An innovative method relating asphalt permittivity to density," *Geosciences*, Vol. 9, No. 7, 280, 2019.

[6] Cao, Q. and I. L. Al-Qadi, "Development of a numerical model to predict the dielectric properties of heterogeneous asphalt concrete," *Sensors*, Vol. 21, No. 8, 2643, 2021.

[7] Zhang, C. and H. Wang, "A new method for compaction quality evaluation of asphalt mixtures with the intelligent aggregate (IA)," *Materials*, Vol. 14, No. 9, 2422, 2021.

[8] Ren, H., Z. Qian, W. Huang, W. Bo, T. Chen, and H. Cao, "Evaluation of fracture behavior in asphalt concrete through the combination of semi-circular bending test and digital image correlation technology," *Construction and Building Materials*, Vol. 451, 138854, 2024.

[9] Chen, Z., "A defect scanning sensor based on a reconfigurable spiral-shaped DGS," *Progress In Electromagnetics Research C*, Vol. 156, 59–65, 2025.

[10] Guattari, C., D. Ramaccia, F. Bilotti, and A. Toscano, "Permittivity of sub-soil materials retrieved through transmission line model and GPR data," *Progress In Electromagnetics Research*, Vol. 151, 65–72, 2015.

[11] Pratticò, D., F. Laganà, G. Oliva, A. S. Fiorillo, S. A. Pullano, S. Calcagno, D. D. Carlo, and F. L. Foresta, "Integration of LSTM and U-net models for monitoring electrical absorption with a system of sensors and electronic circuits," *IEEE Transactions on Instrumentation and Measurement*, Vol. 74, 1–11, 2025.

[12] Versaci, M., F. Laganà, L. Manin, and G. Angiulli, "Soft computing and eddy currents to estimate and classify delaminations in biomedical device CFRP plates," *Journal of Electrical Engineering*, Vol. 76, No. 1, 72–79, 2025.

[13] Laganà, F., D. Pellicanò, M. Arruzzo, D. Pratticò, S. A. Pullano, and A. S. Fiorillo, "FEM-based modelling and AI-enhanced monitoring system for upper limb rehabilitation," *Electronics*, Vol. 14, No. 11, 2268, 2025.

[14] Kaur, S., S. Singh, and M. M. Sinha, "Prototype of circular split ring resonator based sensor for estimating soil moisture as a function of soil particle distribution," *IEEE Sensors Journal*, Vol. 24, No. 19, 29 945–29 952, 2024.

[15] Al Takach, A., F. Ndagijimana, J. Jomaah, and M. Al-Husseini, "Permittivity extraction of moist soil for GPR applications," in *2019 Antennas Design and Measurement International Conference (ADMInC)*, 48–52, St. Petersburg, Russia, 2019.

[16] Joshaghani, A. and M. Shokrabadi, "Ground penetrating radar (GPR) applications in concrete pavements," *International Journal of Pavement Engineering*, Vol. 23, No. 13, 4504–4531, 2022.

[17] Yu, X., R. Luo, T. Huang, J. Wang, and Y. Chen, "Dielectric properties of asphalt pavement materials based on the temperature field," *Construction and Building Materials*, Vol. 303, 124409, 2021.